South African Journal of Chemical Engineering 43 (2023) 135–145

Contents lists available at ScienceDirect

South African Journal of Chemical Engineering

journal homepage: www.elsevier.com/locate/sajce

A significance of multi slip condition for inclined MHD nano-fluid flow with non linear thermal radiations, Dufuor and Sorrot, and chemically reactive bio-convection effect

Bilal Ahmad [a], Muhammad Ozair Ahmad [a], Muhammad Farman [b], Ali Akgül [c,d], Muhammad Bilal Riaz [e,f,*]

[a] Department of Mathematics and Statistics, The University of Lahore, Lahore, Pakistan
[b] Department of Mathematics, Khawaja Fareed University of Engineering and Information Technology, Rahim Yar Khan, Pakistan
[c] Art and Science Faculty, Department of Mathematics, Siirt University, Siirt 56100, Turkey
[d] Near East University, Mathematics Research Center, Department of Mathematics, Near East Boulevard, PC: 99138, Nicosia /Mersin 10, Turkey
[e] Faculty of Applied Physics and Mathematics, Gdansk University of Technology, 80-233 Gdansk, Poland
[f] Department of Mathematics, University of Management and Technology Lahore, 54770 Pakistan

ARTICLE INFO

Keywords:
Numerical modeling
Doufoure and sorret effect
Inclined MHD
Nonlinear radiations
Micro motile organisms
Nanofluid
Multi slip conditions

ABSTRACT

The aim of this research is to discuss the significance of slip conditions for magnetized nanofluid flow with the impact of nonlinear thermal radiations, activation energy, inclined MHD, sorrot and dufour, and gyrotactic micro motile organisms over continuous stretching of a two-dimensional sheet. The governing equations emerge in the form of partial differential equations. Since the resultant governing differential equations are nonlinear, the partial differential equations are transformed into ordinary differential equations using a workable similarity transformation. By using the Bvp4c module of the MATLAB program, the simplified mathematical framework can be numerically solved. The computation of Coefficients of skin friction, Nusselt numbers, different patterns of velocity profiles, fluid temperature, and concentration profiles reveals the physical nature of this study. As compared to earlier investigations, it was found that the obtained results demonstrated high degrees of symmetry and precision. A decline observes in velocity for boosted values of MHD, inclination, and rotatory parameter. However thermal transportation increases by increasing brownien motion, thermophoresis, radiation and Sorrot effect. The study has significant application in heat control systems, food factories, thermal exchangers, biomechanics, biomedical engineering, and aero dynamical systems

1. Introduction

Investigation of heat and mass transportation using stretching geometries and nanofluids must have piqued researcher interest in recent decades due to a slew of engineering applications, including nuclear reactor design, compact heat exchangers, plastic and rubber sheet manufacturing, and cooling of an infinite metallic plate in power, transportation, and electronics. Cooling of any type of high-energy gadget necessitates the use of effective cooling strategies. Due to their low heat transfer qualities, common heat transfer fluids such as water, ethylene glycol, and motor oil have limited heat transfer capabilities. Efficient heat transfer is one of the biggest problems in science today many researchers have worked on it by using modern techniques. Nanofluids are a novel type of heat transfer in fluid, that combines a base fluid with nanoparticles. First time Choi (1998) introduce the concept of nanofluid, as a result, the remarkable change happened in field of heat and mass transfer. A lot of work has been done in the literature, Like Pil Jang and Choi (2007) discuss the effects of various parameters on nano fluid flow. Meyer et al. (2016) discuss the different numerical models of fluid flow. Akbari et al. (2011) studied comparatively of different models of fluid flow like single phase two phase etc. Researchers, like Duangthongsuk and Wongwises (2008), Wang et al. (2022), Cui et al. (2022) developing novelty in heat transportation phenomena.

The diffusion of energy is induced by a composition gradient, which has been empirically demonstrated. The Dufour effect, also known as the diffusion-thermo effect, is a result of this phenomenon. The Soret effect, also known as the thermal diffusion effect, is the process of species diffusion caused by a temperature difference. Furthermore, recent research has revealed that the Dufour and Soret effects are considerable

* Corresponding author.
E-mail addresses: muhriaz@pg.edu.pl, bilalsehole@gmail.com (M.B. Riaz).

https://doi.org/10.1016/j.sajce.2022.10.009
Received 27 April 2022; Received in revised form 18 September 2022; Accepted 28 October 2022
Available online 3 November 2022

Nomenclature

T	non-dimensional temperature	Nb	Brownian motion parameter
T_w	Temperature at surface	ν	Kinematic viscosity
C	non-dimensional nanoparticles concentration	Nt	thermophoresis parameter
C_w	Concentration at surface	ρ_∞	Density of fluid
T_∞	temperature away from the surface	D_T	Thermophoretic diffusion coefficient
E	Activation energy	D_B	Brownian diffusion coefficient
C_∞	concentration away from the surface	ρCp	Base fluid heat capacity
Sc	Schimit number	M	Uniform magnetic field
C_{fx}	skin friction at x-direction	p	pressure
$(u, v,)$	Velocity components	σ_{nf}	Electrical conductivity
C_{fy}	skin friction at y-direction	$(x_1, y_1,)$	Cartesian co-ordinates
u_w	velocity of stretching sheet	λ_1	relaxation time of heat flux
Nu_x	Nusselt number	α	angle of inclination
Sh_x	Sherwood number	β	variable viscosity parameter
		Le	Lewis number parameter
		Pr	Prandtl number.

when heating and mass are transferred in a flow field. Hou et al. (2022) discuss the significance of Dufour and Soret Effects for Pseudo-Plastic Liquid in the presence of Tri-Hybrid Nanoparticles. Naveen Kumar et al. (2022) also investigate the effectiveness of Dufour and Soret Effects over B-fluid with stefan blowing effect under the convective boundary conditions. Akbar et al. (2022) explore the Soret and Dufour effect for Williamson fluid flow in the presences of Mixed convection MHD over non-linear starched surface. Ali et al. (2021) investigate the Soret and Dufour effect with double diffusion on rotating fluid over stretching sheet. Many researchers like Nawaz et al. (2012), Pal and Mondal (2011), Ahmad et al. (2021a) also explore the effects of Soret and Dufour over different domains.

In the development of industrial procedures, thehrinking sheet is used extensively. Mahabaleshwar et al. (2022) discuss the nano fluid flow for shrinking and stretching sheet. Ismail et al. (2022) studied the stability analysis of shrinking sheet in the presence of MHD. Nadeem et al. (2022) discuss the fuzzy parameters in shrinking sheet with MHD effects of nanofluid flow. Ahmad et al. (2021b), Khan et al. (2022b), Ghosh et al. (2022) are also explore the shrinking effects of sheet. Injection and Suction is also having important effect which has creating in result of shrinking/stretching. Gumber et al. (2022) discuss the effect of injection/suction of hybrid micro-polar nanofluid over vertical sheet. Soumya et al. (2022) studied the effect of shapes and injunction/suction nanofluid flow in suction/injection process with nonlinear-thermal-radiation and slip conditions. Khan et al. (2022a) explore the steady squeezing flow of Magnetohydrodynamics Hybrid Nanofluid Flow comprising carbon Nanotube-Ferrous Oxide/Water with Suction/Injection Effect. The recent trends indicated the significance of nanofluid and hybrid nano fluids like Bhatti et al. (2022a,b) Bhatti et al. discuss the application of nano and hybrid nano fluid in solar collectors.

The term (MHD) “magnetohydrodynamic” refers to the behavior of fluid flow when it is subjected to magnetic and electromagnetic forces. Highly conductive boilers, solar panels, and the polymer industry are among the applications that utilize the MHD. Researchers have done a wide range of studies in this sector, with the goal of keeping nanofluids under the influence of electromagnetism. Al-Farhany et al. (2022) studied the effect of MHD effects on nanofluid with u-shape particles effect. Hossain et al. (2022) discuss the effects of MHD and heat flux with

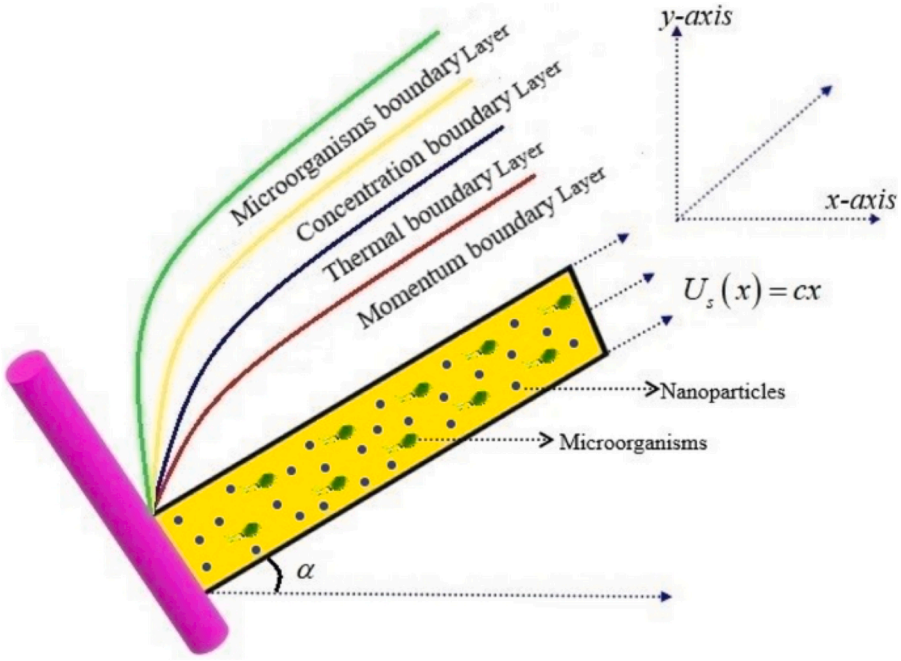

Fig. 1. Inclined MHD nano fluid flow geometry with Bio Convective Particles.

unsteady mixed convection for nanofluid flow through nano carbon tubes. Dezfulizadeh et al. (2022) discuss the energy efficiency with MHD effects for hybrid nanofluid flow over sheet. Alsaedi et al. (2022) studied the numerical simulation with for nanofluid flow with MHD effects. Many researchers Khashi'ie et al. (2022), Gouran et al. (2022), Nemati et al. (2022) explor the effect of MHD effects for fluid flow over different geometries.

In the literature, we observed less attention paid to the importance of magnetized nanofluid with slip conditions for heat exchanging in the presence of nonlinear thermal radiations and motiel micro organism. In current research, we investigate the role of slip conditions with nonlinear radiation, micro motile organisms, chemical reactions, incline MHD, Soret, and DuFour effects on nanofluid flow through a two-dimension porous sheet. Mostly, the nonlinear partially differential equations are appears when we are solving the flow problems. Since the resultant governing differential equations are nonlinear, the partial differential equations are transformed into ordinary differential equations using a workable similarity transformation. The concluding nonlinear governing equations were numerically solved using bvp4c one of the MATLAB functions. As compared to earlier investigations, it was found that the obtained results demonstrated high degrees of symmetry and precision. The outputs are represented tabularly and graphically. The variations of parameters are discussed for velocity profile, temperature profile, concentration profile, and micro motile profile. The findings and comments reported in this paper might aid in a better understanding of nonlinear radiative and inclined MHD nanofluid flow through a porous medium across a stretched sheet.

In this research Section 1 is introduction. Section 2 is development of mathematical model as a result partial differential equations appear as governing equations with slip boundary conditions which converted into ordinary differential equations by using similarities. In Section 3 which is numerical procedure, a numerical method shooting technique apply to get the numerical results. In Section 4 comparison takes place under closed environment to validate the devolved model. In Section 5 obtained results are discussed graphically and in tables also. Conclusion of study drawn in the Section 6 after that future work also discuss.

2. Mathematical model

In this study, we consider the flow of nano fluids through nonlinear porous sheets under inclined magnetohydrodynamics (MHD), magnetized dissipation of dufour and soret, joule heating, and bioconvection with moment, thermal, concentration, and micro motile slip boundary conditions. There is a nonuniform velocity $U(x,t)=\frac{ax}{1-\lambda t}$ along the x-axis of the sheet.

The geometry of flow is shown in the Fig. 1. The sheet is extended across the fluid flow with theixed origin given the impact of opposing forces. The flow ttern proceeded cording to the sheet's stretching along the x-axis. According to above assumptions and boundary conditions, the governing equations of steady state conditions are given below.

$$u_x+u_y=0, \tag{1}$$

$$uu_x+vv_y=\nu u_{y_y}-\frac{\nu}{K}u-\frac{\sigma B^2 sin\alpha}{\rho}u+\frac{g}{\rho_f}(1-C_\infty)\rho f_\infty\beta(T-T_\infty)-\left(\rho_p-\rho f_\infty\right)(C-C_\infty)(N-N_\infty), \tag{2}$$

$$uT_x+vT_y=\frac{k}{\rho c_p}T_{yy}+\left[D_bC_yT_y+\frac{D_T}{T_\infty}\left(T_y\right)^2\right]+\frac{\mu}{\rho c_p}\left(u_y\right)^2+\frac{Dk_t}{c_sc_p}C_{yy}, \tag{3}$$

$$uC_x+vC_y=D_mC_{yy}-K_1(C-C_\infty)+\frac{D_mk_T}{T_m}T_{yy}+D_bC_{yy}+\frac{D_T}{T_\infty}T_{yy}, \tag{4}$$

$$uN_x+vN_y+\frac{bW_c}{C_w-C_\infty}.\left[\frac{\partial}{\partial y}\left(NC_y\right)\right]=D_mN_{y_y}. \tag{5}$$

The q_r radiative flux of radiation is shape up as follows

$$q_r=-T^3T_y\frac{16\sigma}{3k} \tag{6}$$

The velocity components are representing by u, v, and w, $\nu=\left(\frac{\mu}{\rho}\right)$ representation of kinematic viscosity, μ used for dynamic viscosity, K used for permeability of the porous medium, C_b indicate the drag coefficient,k is the thermal conductivity, and c_p is a representation of specific heat, D_T are the thermophoretic coefficient, D_m representation of microorganism coefficient, $\frac{\sigma B^2 sin\alpha}{\rho}$ representation of inclined MHD.

The boundary conditions are:

$$\begin{cases} u=U(x,t)+U_slip, v=v_w, -\kappa T_y=h_f\left(T_f-T\right), \\ -D_BC_y=h_s(C_s-C), N=N_w(x,t)=N_slip, N=-mu_yaty=0, \\ u\longrightarrow 0, v\longrightarrow 0, T\longrightarrow T_\infty, C\longrightarrow C_\infty, N\longrightarrow N_\infty wheny\longrightarrow\infty. \end{cases} \tag{7}$$

Where T_w is the wall temperature, T_∞ ambient temperature, C_w is the concentration well beyond the wall, C_∞ is ambient concentration

The similarity transformations previously defined as

$$\begin{cases} u=axf^{'}(\eta), v=axg(\eta), \eta=\sqrt{\frac{a}{\nu}}.z, \\ \chi(\eta)(N_w-N_\infty)=N-N_\infty, w=-(a\nu)^{\frac{1}{2}}. \end{cases} \tag{8}$$

By above mentioned similarities transformations Eq. (5) is inconsequential verified, and Eqs. (6)–(10) above-mentioned model will yield the following results

$$f^{'''}+f.f^{''}-Mf^{'}-f^{'2}+G_r(\theta-N_r\phi-R_b\psi)=0, \tag{9}$$

$$\begin{cases} \frac{1}{P_r}(1+4/3R_d)\theta^{''}+f\theta^{'}+Ecf^{''2}+N_b\theta^{'}\phi^{'}+N_t\theta^{'2}+4\Big/3\left[(\theta_w-1)^3\left(3\theta^{'2}\theta^2+\theta^3\theta^{''}+\right.\right. \\ \left.\left.3(\theta_w-1)^2\right)\left(2\theta^{'2}\theta+\theta^2\theta^{''}\right)+3(\theta_w-1)\left(\theta^{'2}+\theta\theta^{''}\right)\right]=0, \end{cases} \tag{10}$$

$$\phi^{''}+S_c.f.\phi^{'}+S_cS_r\theta^{''}+\frac{N_t}{N_b}\theta^{''}=0, \tag{11}$$

$$\chi^{''}+P_rL_b\chi^{'}-P_e(\phi^{''}(\sigma+\chi)+\chi^{'}\phi^{'})=0. \tag{12}$$

Now the transferred boundary conditions are

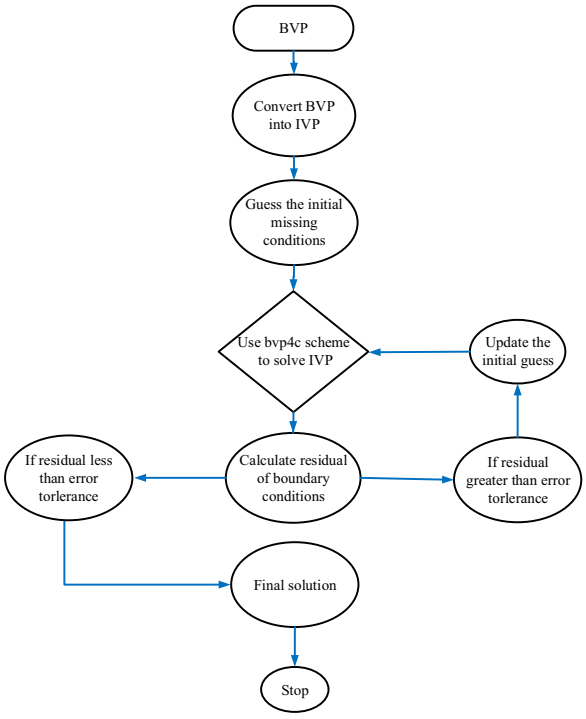

Fig. 2. Methodology flow Chart.

Skin friction coefficient C_{fx}, Nusetl number N_{ux}, Sherwood number S_{hx}, and Micro motile density number N_{nx}, are already defined as in literature by many researchers like, Begum et al. (2017), Pal and Mondal (2022), Jalil et al. (2017)

$$C_{fx} = \frac{\tau_w}{\rho U_w^2}, \tag{14}$$

$$N_{ux} = \frac{xq_w}{k(T_w - T_\infty)}, \tag{15}$$

$$S_{hx} = \frac{xq_m}{D(C_m - C_\infty)}, \tag{16}$$

$$N_{nx} = \frac{xq_n}{D_m(N_w - N_\infty)}. \tag{17}$$

In Eqs (14), (15), (16), (17) τ_w is the value of shear stress, q_w is the value of local heat flux, q_m is the value of local mass flux, and q_n is the value of micro motile flux which are equal

$$\tau_w = \mu u_y(0), \tag{18}$$

$$q_w = -KT_y(0), \tag{19}$$

$$q_m = -DC_y(0), \tag{20}$$

$$q_n = -D_n N_y(0). \tag{21}$$

after the using of above value the non dimensional values of Skin friction, Nustel number, Sherwood number, and Micro motile number are

$$\begin{cases} f = f_w, f' = 1 + S_f f'', g = -mf'', \theta = N_c[1 - \theta 0], \phi = -N_d[1 - \phi'], \chi = 1 + S_g \chi', at\eta = 0, \\ f' \longrightarrow 0, g \longrightarrow 0, \chi \longrightarrow 0, \theta \longrightarrow 0, \phi \longrightarrow 0, at\eta \longrightarrow \infty. \end{cases} \tag{13}$$

After using the above similarities and after simplification of above model following dimensionless numbers are appeared, which are denoted as, $M = \frac{\sigma B^2 \sin\alpha}{\rho}$ known as Hartman number, $N_d = \frac{D_{Tc} C_o}{\nu T_o}$ known as Dufour number, $S_r = \frac{\nu}{D_s}$ known as soret number, $E_c = \frac{a^2}{c_p(T_w - T_\infty)}$ known as Eckert number, $Gt = \frac{\rho g x^3 \beta_T (T_w - T_\infty)}{\nu^2}$ known as local thermal Grashoof number, $R_(ex) = \frac{x.U}{\nu}$ known as local Reynolds number, $P_r = \frac{\nu}{\alpha}$ known as Prandtl number, $N_r = \frac{\rho_p - \rho_f(C_w - C_f)}{\rho_f \beta (1 - C_\infty)(T_w - T_\infty)}$ known as buoyancy ration value, $R_b = \frac{\rho_p - \rho_f(N_w - N_f)}{\rho_f \beta (1 - C_\infty)(T_w - T_\infty)}$ known as bio convective Reyligh number, $S_c = \frac{\nu}{D_b}$ known as schmidt number, $P_e = \frac{bW_c}{dm}$ known as Pecelt number, $\theta_w = \frac{T_w}{T_\infty}$ known as temperature ration value, $N_b = \frac{\tau D_b (C_w - C_\infty)}{\nu}$ known as value of Brownian motion, $N_t = \frac{\tau D_b (T_w - T_\infty)}{T_\infty \nu}$ known as value of Thermophoresis, $Gr = \frac{G_t}{R_{ex}^2}$ is known as thermal Grashoof number.

converted

$$C_{fx} Re_x = f''(0), \tag{22}$$

$$N_{ux} Re_x = \theta'(0), \tag{23}$$

$$S_{hx} Re_x = \phi'(0), \tag{24}$$

$$N_{nx} Re_x = \chi'(0). \tag{25}$$

where the Re_x is called Reynolds number $Re_x = \frac{ax^2}{\nu}$

3. Numerical procedure

The exact solution to the current problem seems to be complicated. Therefore MATLAB is being used to solve the problem by discussing below numerical procedure. The bvp4c methodology is used to solve the

Table 1
Comparison of temperature profile $\theta'(0)$ with distinct values of different parameters with Begum et al. (2017) and Pal and Mondal (2022) results.

Nt	Begum et al. (2017)		Pal and Mondal (2022)		Current Findings	
	Nb = 0.2	Nb = 0.6	Nb = 0.2	Nb = 0.6	Nb = 0.2	Nb = 0.6
0.2	0.092906	0.038324	0.092894	0.038319	0.092784	0.038301
0.4	0.092731	0.032497	0.092700	0.032495	0.092679	0.032483
0.6	0.092545	0.026905	0.092507	0.026913	0.092499	0.026904
0.8	0.092343	0.022010	0.092316	0.022045	0.092298	0.022048
0.9	0.092126	0.018034	0.092123	0.018095	0.092125	0.018101

Table 2
Comparison of temperature profile $\theta'(0)$ with distinct values of different parameters with Begum et al. (2017) and Pal and Mondal (2022) results.

M	Cui et al. (2022)		Mahabaleshwar et al. (2022)		Current Findings	
	$-f''(0)$	$\theta'(0)$	$-f''(0)$	$\theta(0)'$	$-f''(0)$	$\theta'(0)$
0.0	1.000000	0.0000	1.0000080	0.00000	1.0000153	0.000000
0.2	1.095445	0.5128	1.0954458	0.51282	1.0954621	0.512772
0.6	1.224745	0.8371	1.2247446	0.83714	1.2247486	0.837101
1.0	1.414214	1.2873	1.4142132	1.28736	1.4142152	1.287253

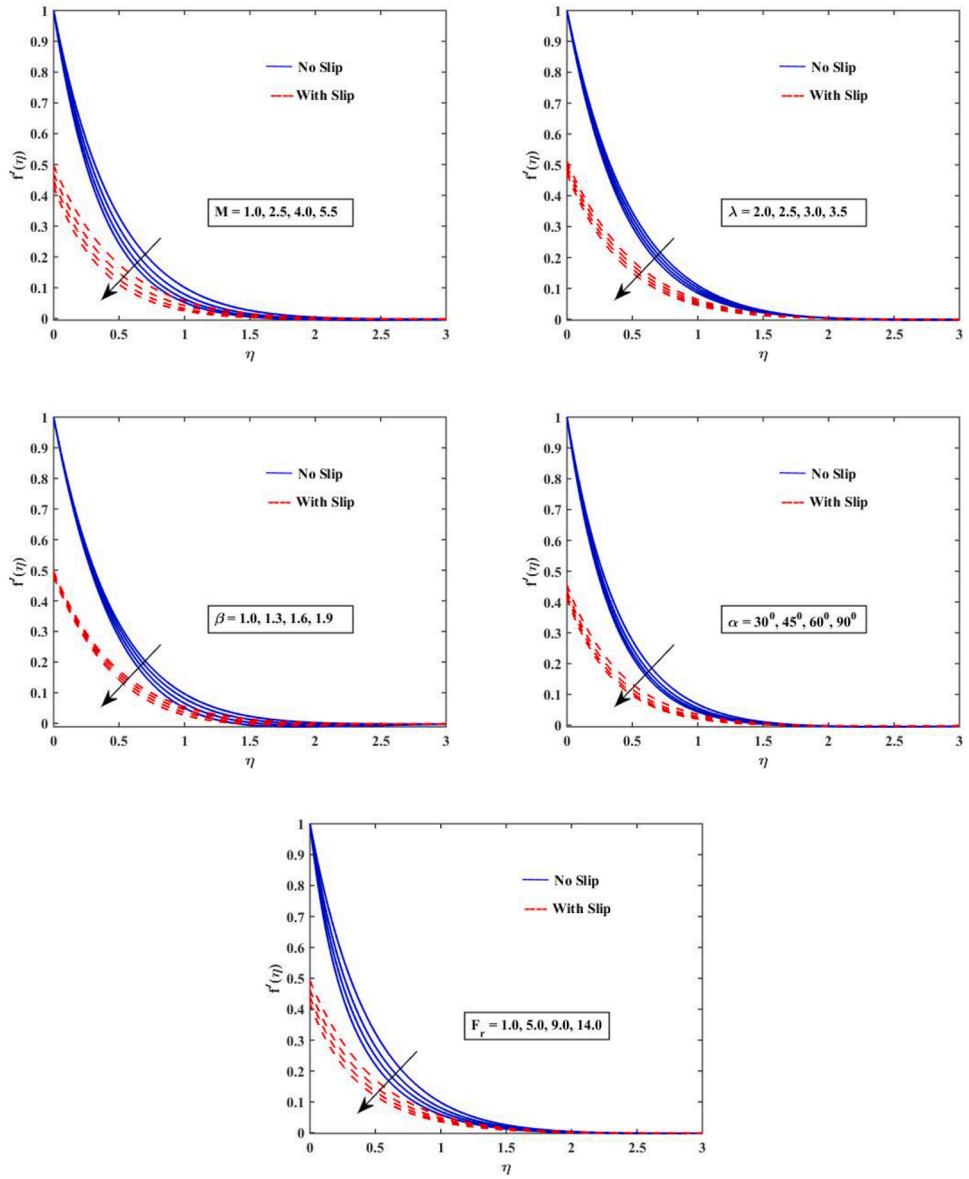

Fig. 3. Fluctuation in Velocity Profile $f'(\eta)$ along different parameters.

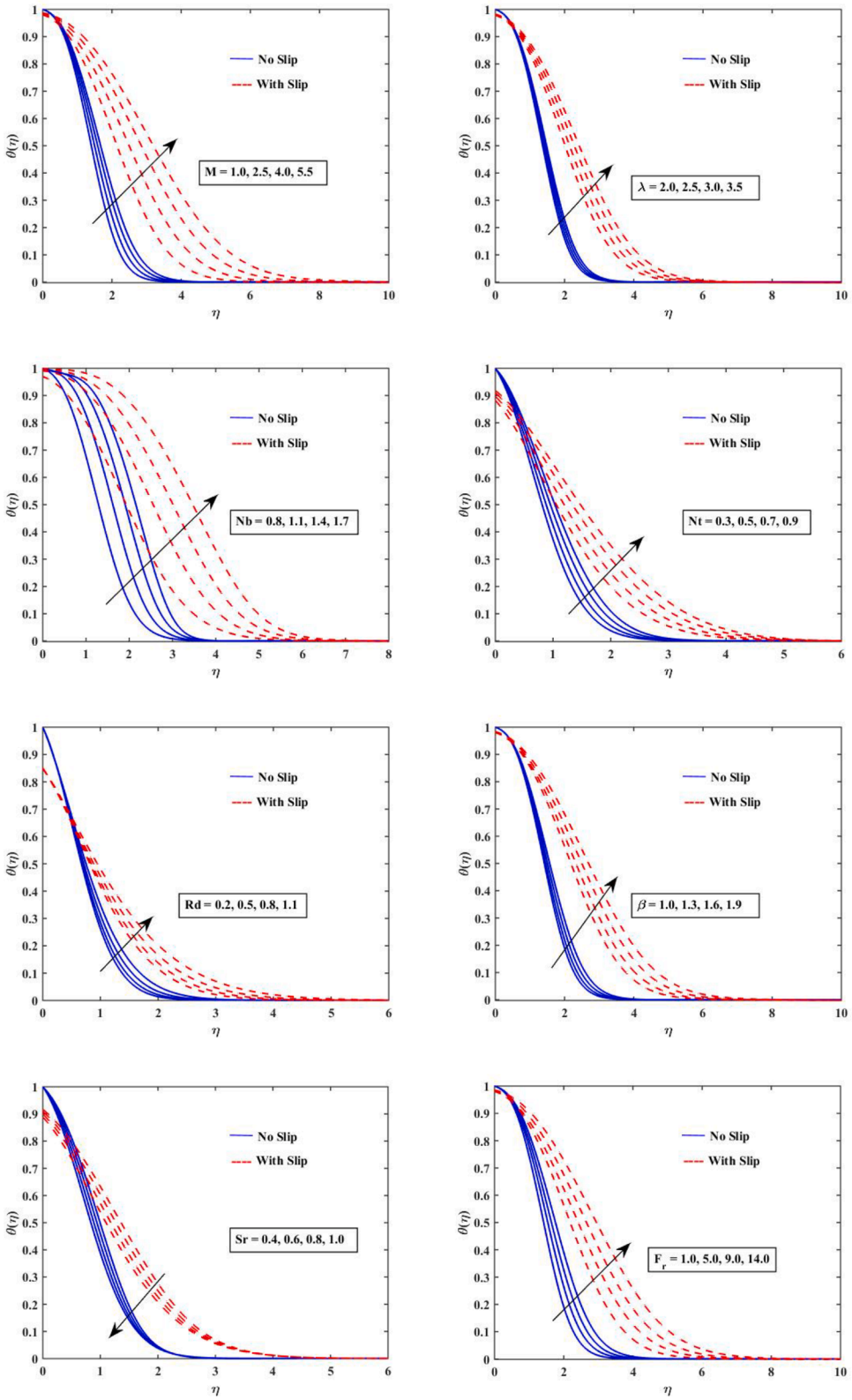

Fig. 4. Fluctuation in Temperature Profile $\theta(\eta)$ along different parameters.

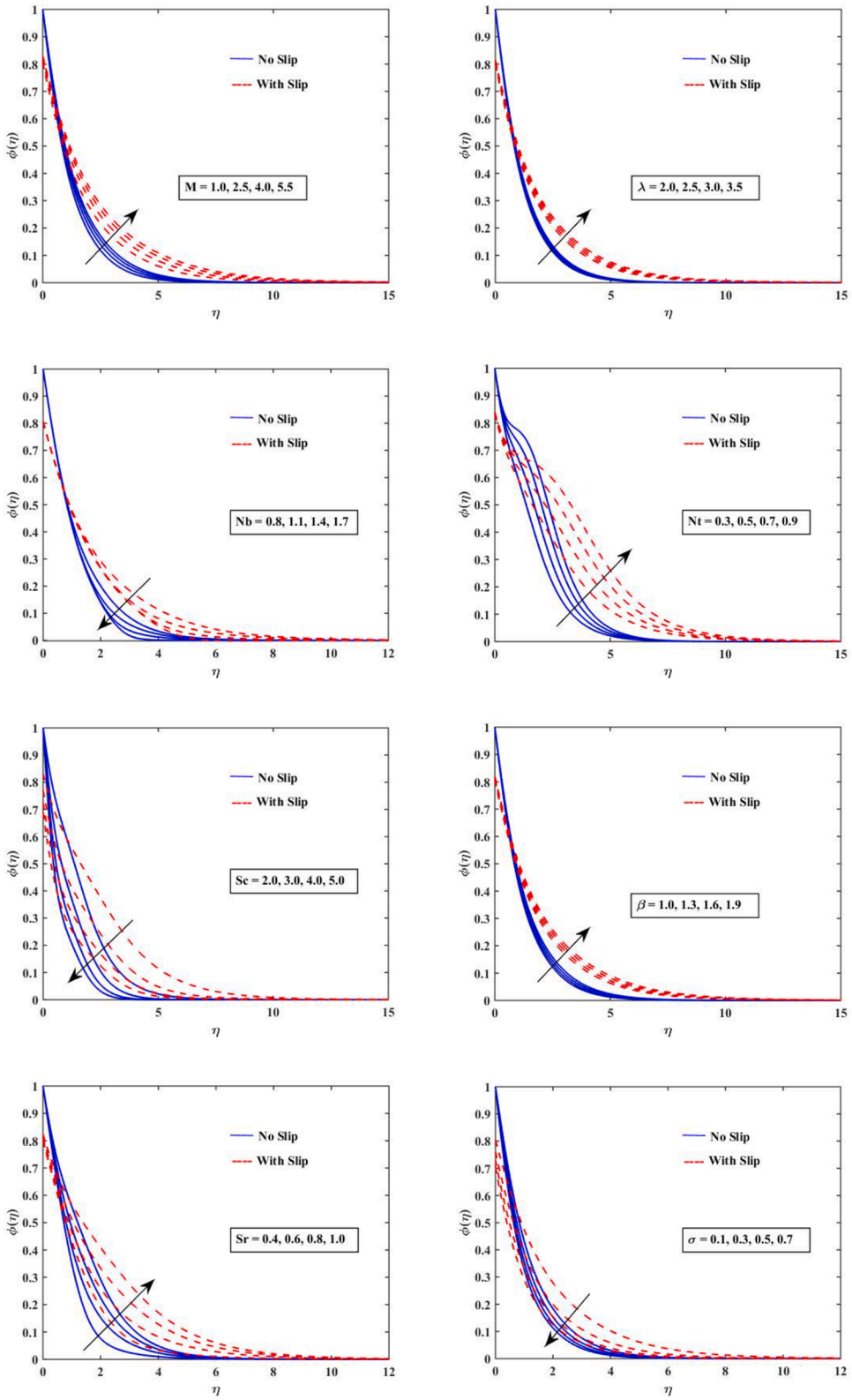

Fig. 5. Fluctuation in Concentration Profile $\Phi(\eta)$ along different parameters.

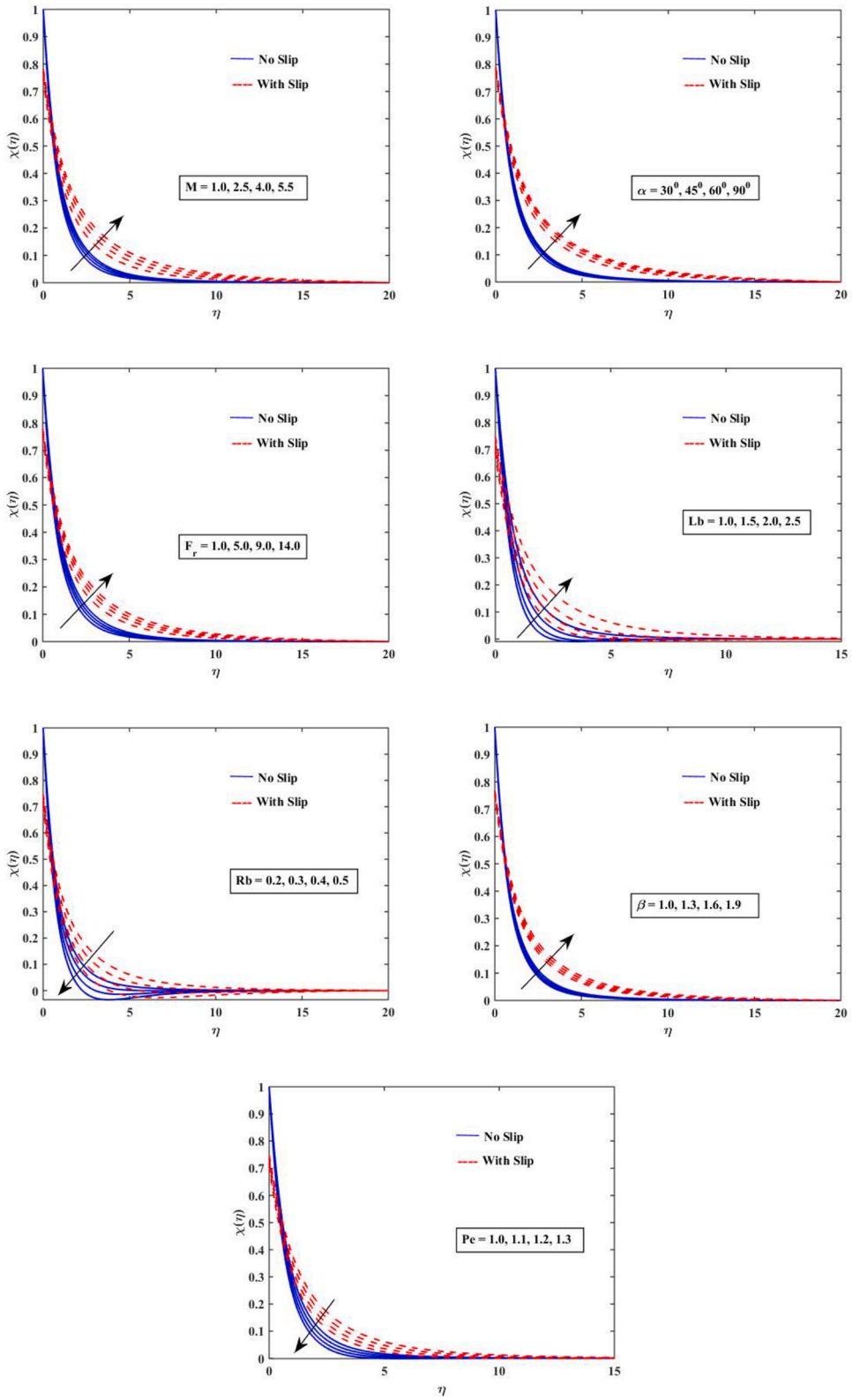

Fig. 6. Fluctuation in Micro Organism Profile $\chi(\eta)$ along different parameters.

Table 3
Numerical results for coefficient of skin friction, Nusselt number, Sherwood Number, and Micro Motile Number of nanofluid and for slip effect with different parameters.

M	S_c	G_r	Nt	Nb	$-Cf_x$	$-Nu_x$	$-Sh_x$	$-Nh_x$
1.0	0.2	1.0	0.1	0.1	3.134021	0.6225744	0.5331885	0.7062711
1.5					3.335692	0.5630240	0.5561623	0.6781460
2.0					2.908412	0.5136472	0.5771311	0.6594955
2.5					2.871653	0.4733730	0.5946434	0.6462538
	0.2				1.5872715	0.6225743	0.5331885	0.7062711
	0.5				1.6536586	0.6209624	0.5344349	0.7070119
	0.8				1.7219583	0.6166805	0.5365094	0.7060292
	1.1				1.791174	0.6223866	0.539129	0.703833
		1.0			1.5872715	0.6225744	0.5331885	0.7062711
		2.0			1.7784707	0.5975564	0.5428274	0.6942725
		3.0			1.9535947	0.5740727	0.5521910	0.6836087
		4.0			2.1164658	0.5510572	0.5616085	0.6737208
			0.1		1.5872715	0.6225744	0.5331885	0.7062711
			0.3		1.5872715	0.5430147	0.1317556	0.4966811
			0.5		1.5872715	0.4741037	-0.0692192	0.3973130
			0.7		1.5872715	0.4146559	-0.1215313	0.3772477
				0.2	1.5872715	0.5599217	0.7080255	0.8002808
				0.4	1.5872715	0.4485822	0.7932986	0.8461412
				0.6	1.5872715	0.3549215	0.8199253	0.8603803
				0.8	1.5872715	0.2774614	0.8320147	0.8667833

Table 4
Numerical results for coefficient of skin friction, Nusselt number, Sherwood Number, and Micro Motile Number of nanofluid and for non-slip effect with different parameters.

M	S_c	G_r	Nt	Nb	$-Cf_x$	$-Nu_x$	$-Sh_x$	$-Nh_x$
1.0	0.2	1.0	0.1	0.1	2.333031	0.6225744	0.5331885	0.7062711
1.5					2.572214	0.5630240	0.5561623	0.6781460
2.0					2.787806	0.5136472	0.5771311	0.6594955
2.5					2.835034	0.4733730	0.5946434	0.6462538
	0.2				1.5872715	0.6225743	0.5331885	0.7062711
	0.5				1.6536586	0.6209624	0.5344349	0.7070119
	0.8				1.7219583	0.6166805	0.5365094	0.7060292
	1.1				1.791174	0.6223866	0.539129	0.703833
		1.0			1.5872715	0.6225744	0.5331885	0.7062711
		2.0			1.7784707	0.5975564	0.5428274	0.6942725
		3.0			1.9535947	0.5740727	0.5521910	0.6836087
		4.0			2.1164658	0.5510572	0.5616085	0.6737208
			0.1		1.5872715	0.6225744	0.5331885	0.7062711
			0.3		1.5872715	0.5430147	0.1317556	0.4966811
			0.5		1.5872715	0.4741037	-0.0692192	0.3973130
			0.7		1.5872715	0.4146559	-0.1215313	0.3772477
				0.2	1.5872715	0.5599217	0.7080255	0.8002808
				0.4	1.5872715	0.4485822	0.7932986	0.8461412
				0.6	1.5872715	0.3549215	0.8199253	0.8603803
				0.8	1.5872715	0.2774614	0.8320147	0.8667833

system of ordinary differential Eqs. (13)–(17) of fluid flow model. The tolerance of given problem is 10^{-7} and the more details of methodology see in below figure. To compute the result, the first guess is necessary to meet the boundary condition when using this approach. For the implementation following variables are introduced (Fig. 2).

$$\begin{cases} f=\zeta_1, f'=\zeta_2, f''=\zeta_3, f'''=\zeta.\zeta_1, \\ \theta=\zeta_4, \theta'=\zeta_5, \theta''=\zeta.\zeta_2, \\ \phi=\zeta_6, \phi'=\zeta_7, \phi''=\zeta.\zeta_3, \\ \chi=\zeta_8, \chi'=\zeta_9, \chi''=\zeta.\zeta_4. \end{cases} \tag{26}$$

$$\zeta.\zeta_1=\frac{1}{1-\beta}.{\zeta_2}^2-2\beta.\zeta_4+\lambda.\zeta_2-\zeta_1.\zeta_3, \tag{27}$$

$$\zeta.\zeta_2=-P_r\left(\zeta_1.\zeta_7+\left(N_b\zeta_7.\zeta_9+N_t{\zeta_7}^2\right)\right), \tag{28}$$

$$\zeta.\zeta_3=S_c\sigma(1+\delta.\zeta_6)^n.e^{\frac{-E}{1+\sigma.\zeta_6}}.\zeta_8-S_c.\zeta_1.\zeta_9, \tag{29}$$

$$\zeta.\zeta_4=P_e(\zeta.\zeta_4.(\sigma+\zeta_{10})+\zeta_1 1.\zeta_9)-P_r.L_b.F.\zeta_{11}. \tag{30}$$

$$\begin{cases} \zeta_1=f_w, \zeta_2=1+S_f\zeta_3, \zeta_4=1+\zeta_5 S_\theta, \zeta_6=1+1+\zeta_7 S_\chi, at\eta=0. \\ \zeta_2\longrightarrow 0, \zeta_4\longrightarrow 0, \zeta_6\longrightarrow 0, \zeta_8\longrightarrow 0, \zeta_{10}\longrightarrow 0, at\eta\longrightarrow 0. \end{cases} \tag{31}$$

4. Model validity

We showed and analyzed the findings of the above-mentioned technique in this section. When recent findings are matched to prior findings of Begum et al. (2017), Pal and Mondal (2022), Jalil et al. (2017), Abdal et al. (2019), for limited cases, the validity of the obtained results are proven. The outcomes due to variations of viscosity, Inclined MHD, micro motility, and Arrhenius energy are explored in tables and figures by using the default numeric values of parameters that are already dimensionless in the mathematical model, $N_t=0.1$, $N_b=0.2$, M $=1$, $\gamma=0.1$, $\theta_w=0.1$, Ec $=0.1$, $\beta=0.5$, Rd $=0.1$, Pr $=0.7$, Sc $=0.1$, Kr $=0.1$, Sr $=0.1$, Rb $=0.2$, Nr $=0.2$, Lb $=1$, $\sigma=0.5$, Pe $=0.1$, Nc $=0.2$, $\lambda=0.01$, $\alpha=30^\circ$, s $=0.2$, A $=1$, B $=1$, C $=1$, D $=1$. These comparison tables comprehensively showing the validation with exciting literature (Tables 1 and 2).

5. Result and discussion

This section explain the results and effectiveness of current study for the velocity profile, temperature profiles, nano particle concentration profiles, and density of motile micro organisms profiles. These results are find out under fix values of parameters: $= 25^o; \beta = 0:8; \lambda = 2.1; Fr = 0.3; Pr = 1.9; Sc = 2.2; \sigma = 0.2; E = 1.4; Sr = 0.2; Nb = 0.8; Nt = 0.4; Lb = 1.3; Pe = 1.2; Rb = 0:4; M = 1.4; Rd = 0:3$. The fascinating factor of current research is comparison of two different types of boundary conditions, one is non-slip and other is multi-slip boundary conditions.

In the first set of the figures describe the effect of different parameters on velocity profile $f'(\eta)$. In Fig. 3, the consequences observe that for the boosted values of the parameters, MHD parameter M, parameter of porosity λ, angle of inclination α, rotating parameter β, Eclet number Fr velocity showing decreasing behavior. Lorentz forces create the hindrance in the fluid flow which reduces the velocity of fluid. In the Fig. 4, the behavior of temperature profile discuss. it is clearly observed the enlargement in temperature profile for the boosted values of λ, M, β, Nb, Nt, Rd, and Sr. it shows decreasing behavior for the boosted value of Sr In the Fig. 5, the behavior of concentration profile discuss. it is clearly observed the enlargement in concentration profile for the boosted values of λ, M, β, Nb, Nt, Rd, and Sr. it shows decreasing behavior for the boosted value of Sr, Sc, and σ. In the Fig. 6, the behavior of motile micro organism profile discuss. it is clearly observed the enlargement in motile micro organism profile for the boosted values of λ, M, β, Nb, Nt, Rd, and Sr. it shows decreasing behavior for the boosted value of Sr, Sc, and σ.

In the below Table 3 the values of skin friction, Nussetl number, sherwood number and motile micro organism number are concluded under the boosted values of few parameters for the suction phenomena. The values of skin friction coefficient increases with increasing of value of M, Rayleigh number R_b, Natural convicting numberN_r and remain constant for the value of Nt and Nb, and decreases by increasing the value of Grashoof number G_r, Pecalt numberP_e, Prandel numberP_r. The nustel number depreciation observed for the boosted values of M, and increasing for the boosted value of, Grashoof number G_r, Pecalt numberP_e, Nt and Nb. The values of Sherwood number for the boosted values of Grashoof number G_r, Pecalt numberP_e, N_t, and N_b, and decreases for the value of M. The motile micro organism number increment observed for the the boosted values of Grashoof number G_r, Lewis numberL_e, N_t, N_b, Pecalt numberP_e and decreases for boosted value of M.

In the below Table 4 the values of skin friction, Nussetl number, sherwood number and motile micro organism number are concluded under the boosted values of few parameters for the suction phenomena. The values of skin friction coefficient increases with increasing of value of M, Rayleigh number R_b, Natural convicting numberN_r and remain constant for the value of Nt and Nb, and decreases by increasing the value of Grashoof number G_r, Pecalt numberP_e, Prandel numberP_r. The nustel number depreciation observed for the boosted values of M, and increasing for the boosted value of, Grashoof number G_r, Pecalt numberP_e, Nt and Nb. The values of Sherwood number for the boosted values of Grashoof number G_r, Pecalt numberP_e, N_t, and N_b, and decreases for the value of M. The motile micro organism number increment observed for the the boosted values of Grashoof number G_r, Lewis numberL_e, N_t, N_b, Pecalt numberP_e and decreases for boosted value of M.

6. Conclusion

In Current research, we studied the two-dimension Nanofluid through a porous medium containing Inclined magneto hydrodynamics force, nonlinear radiations, sort and Dufour effect,bio-convection, joule heating, chemical reaction, and suction injection parameter. The dimensionless fluid flow governing equations are numerically solved with help of the bvp4c package of MATLAB. The obtaining results are shown graphically and tabularly for slip and non-slip conditions. The comparison of obtained results is also showing significance with few other existing results in the literature for the biconvection flow in Nanofluid which endorse the applicable value of bioconvection pattern. Few important results are given below

- The velocity profile along f' has negative behavior for the boosted values of β and inclined M for both suction and injection.
- The temperature profile of nanofluid is enhanced for the boosted value of Nb and Nt and having the decreasing behavior nature for the large value of Pr for both Suction and injection.
- The concentration of nanofluid is increasing for the boosted value of λ, Nt, E and observe opposite behavior for Sc, Nb, M
- The profile of micro motile organism is increasing nature for the enhanced value of Pe and observe decreasing behavior for the boosted value of λ
- The values of skin friction coefficient increases with increasing of rotatory parameter R_b, porosity parameter λ, and remain constant for the value of Nt and Nb.
- The motile micro organism number increment observed for the the boosted values of M, porosity parameter λ, and Nt and Nb.

Future work

The parametric implications of fluid dynamics have been effectively clarified through our computational work. This research work might be expanded in different directions.

- Maxwell, williamson, prandel, and viscoelastic Jeffrey's nanofluids might incorporate.
- Three dimensional sheet, cylinder, disc might incorporate for fluid flow.

Declaration of Competing Interest

The authors declare that they have no conflict of interest.

References

Abdal, S., Ali, B., Younas, S., Ali, L., Mariam, A., 2019. Thermo-diffusion and multislip effects on MHD mixed convection unsteady flow of micropolar nanofluid over a shrinking/stretching sheet with radiation in the presence of heat source. Symmetry 12 (1), 49.
Ahmad, B., Perviz, A., Ahmad, M.O., Dayan, F., 2021. Numerical solution with non-polynomial cubic spline technique of order four homogeneous parabolic partial differential equations. Sci. Inq. Rev. 5 (4).
Ahmad, B., Perviz, A., Ahmad, M.O., Dayan, F., 2021. Solution of parabolic partial differential equations via non-polynomial cubic spline technique. Sci. Inq. Rev. 5 (3).
Akbar, T., Ahmed, K., Muhammad, T., Munir, S., 2022. Physical characteristics of dufour and soret effects on MHD mixed convection flow of williamson fluid past a nonlinear stretching porous curved surface. Waves Random Complex Media 1–18.
Akbari, M., Galanis, N., Behzadmehr, A., 2011. Comparative analysis of single and two-phase models for CFD studies of nanofluid heat transfer. Int. J. Therm. Sci. 50 (8), 1343–1354.
Al-Farhany, K., Abdulkadhim, A., Hamzah, H.K., Ali, F.H., Chamkha, A., 2022. MHD effects on natural convection in a u-shaped enclosure filled with nanofluid-saturated porous media with two baffles. Prog. Nucl. Energy 145, 104136.
Ali, B., Hussain, S., Nie, Y., Hussein, A.K., Habib, D., 2021. Finite element investigation of Dufour and Soret impacts on MHD rotating flow of Oldroyd-B nanofluid over a stretching sheet with double diffusion Cattaneo Christov heat flux model. Powder Technol. 377, 439–452.
Alsaedi, A., Muhammad, K., Hayat, T., 2022. Numerical study of MHD hybrid nanofluid flow between two coaxial cylinders. Alex. Eng. J. 61 (11), 8355–8362.
Begum, N., Siddiqa, S., Hossain, M., 2017. Nanofluid bioconvection with variable thermophysical properties. J. Mol. Liquids 231, 325–332.
Bhatti, M., Öztop, H.F., Ellahi, R., Sarris, I.E., Doranehgard, M., 2022. Insight into the investigation of diamond (C) and Silica (SiO2) nanoparticles suspended in water-based hybrid nanofluid with application in solar collector. J. Mol. Liq. 357, 119134.
Bhatti, M.M., Bég, O.A., Abdelsalam, S.I., 2022. Computational framework of magnetized MgO–Ni/water-based stagnation nanoflow past an elastic stretching surface: application in solar energy coatings. Nanomaterials 12 (7), 1049.
Choi, S.U.-S., 1998. Nanofluid Technology: Current Status and Future Research. Technical Report. Argonne National Lab.(ANL), Argonne, IL (United States).
Cui, W., Cao, Z., Li, X., Lu, L., Ma, T., Wang, Q., 2022. Experimental investigation and artificial intelligent estimation of thermal conductivity of nanofluids with different nanoparticles shapes. Powder Technol. 398, 117078.

Dezfulizadeh, A., Aghaei, A., Hassani Joshaghani, A., Najafizadeh, M.M., 2022. Exergy efficiency of a novel heat exchanger under MHD effects filled with water-based Cu–SiO2-MWCNT ternary hybrid nanofluid based on empirical data. J. Therm. Anal. Calorim. 147 (7), 4781–4804.
Duangthongsuk, W., Wongwises, S., 2008. Effect of thermophysical properties models on the predicting of the convective heat transfer coefficient for low concentration nanofluid. Int. Commun. Heat Mass Transf. 35 (10), 1320–1326.
Ghosh, S., Mukhopadhyay, S., Vajravelu, K., 2022. Hybrid nanofluid flow close to a stagnation point past a porous shrinking sheet. Waves Random Complex Media 1–17.
Gouran, S., Mohsenian, S., Ghasemi, S., 2022. Theoretical analysis on MHD nanofluid flow between two concentric cylinders using efficient computational techniques. Alex. Eng. J. 61 (4), 3237–3248.
Gumber, P., Yaseen, M., Rawat, S.K., Kumar, M., 2022. Heat transfer in micropolar hybrid nanofluid flow past a vertical plate in the presence of thermal radiation and suction/injection effects. Partial Differ. Eqs. Appl.Math. 5, 100240.
Hossain, R., Azad, A., Hasan, M.J., Rahman, M., 2022. Thermophysical properties of kerosene oil-based CNT nanofluid on unsteady mixed convection with MHD and radiative heat flux. Eng. Sci. Technol.Int. J. 35, 101095.
Hou, E., Wang, F., Nazir, U., Sohail, M., Jabbar, N., Thounthong, P., 2022. Dynamics of tri-hybrid nanoparticles in the rheology of pseudo-plastic liquid with Dufour and Soret effects. Micromachines 13 (2), 201.
Ismail, N.S., Rahim, Y.F., Arifin, N.M., Nazar, R., Bachok, N., 2022. Stability analysis of the stagnation-point flow and heat transfer over a shrinking sheet in nanofluid in the presence of MHD and thermal radiation. J. Adv. Res. Fluid Mech.Therm. Sci. 91 (2), 96–105.
Jalil, M., Asghar, S., Yasmeen, S., 2017. An exact solution of MHD boundary layer flow of dusty fluid over a stretching surface. Math. Probl. Eng. 2017.
Khan, M.S., Mei, S., Ali Shah, N., Chung, J.D., Khan, A., Shah, S.A., 2022. Steady squeezing flow of magnetohydrodynamics hybrid nanofluid flow comprising carbon nanotube-ferrous oxide/water with suction/injection effect. Nanomaterials 12 (4), 660.
Khan, U., Zaib, A., Ishak, A., Pop, I., 2022. Hybrid nanofluid flow past an unsteady porous stretching/shrinking sheet with newtonian heating in a porous medium. J. Porous Media 25 (5).
Khashi'ie, N.S., Arifin, N.M., Pop, I., 2022. Magnetohydrodynamics (MHD) boundary layer flow of hybrid nanofluid over a moving plate with joule heating. Alex. Eng. J. 61 (3), 1938–1945.
Mahabaleshwar, U., Vishalakshi, A., Andersson, H.I., 2022. Hybrid nanofluid flow past a stretching/shrinking sheet with thermal radiation and mass transpiration. Chin. J. Phys. 75, 152–168.
Meyer, J.P., Adio, S.A., Sharifpur, M., Nwosu, P.N., 2016. The viscosity of nanofluids: a review of the theoretical, empirical, and numerical models. Heat Transf. Eng. 37 (5), 387–421.
Nadeem, M., Siddique, I., Awrejcewicz, J., Bilal, M., 2022. Numerical analysis of a second-grade fuzzy hybrid nanofluid flow and heat transfer over a permeable stretching/shrinking sheet. Sci. Rep. 12 (1), 1–17.
Naveen Kumar, R., Saleh, B., Abdelrhman, Y., Afzal, A., Punith Gowda, R., 2022. Soret and Dufour effects on Oldroyd-B fluid flow under the influences of convective boundary condition with Stefan blowing effect. Indian J. Phys. 1–8.
Nawaz, M., Hayat, T., Alsaedi, A., 2012. Dufour and Soret effects on MHD flow of viscous fluid between radially stretching sheets in porous medium. Appl. Math. Mech. 33 (11), 1403–1418.
Nemati, M., Sani, H.M., Jahangiri, R., Chamkha, A.J., 2022. MHD natural convection in a cavity with different geometries filled with a nanofluid in the presence of heat generation/absorption using lattice Boltzmann method. J. Therm. Anal. Calorimetry 1–15.
Pal, D., Mondal, H., 2011. MHD non-Darcian mixed convection heat and mass transfer over a non-linear stretching sheet with Soret–Dufour effects and chemical reaction. Int. Commun. Heat Mass Transf. 38 (4), 463–467.
Pal, D., Mondal, S.K., 2022. Magneto-bioconvection of Powell Eyring nanofluid over a permeable vertical stretching sheet due to gyrotactic microorganisms in the presence of nonlinear thermal radiation and Joule heating. Int. J. Ambient Energy 43 (1), 924–935.
Pil Jang, S., Choi, S. U., 2007. Effects of various parameters on nanofluid thermal conductivity.
Soumya, D., Gireesha, B., Venkatesh, P., Alsulami, M., 2022. Effect of NP shapes on Fe3O4–Ag/kerosene and Fe3O4–Ag/water hybrid nanofluid flow in suction/injection process with nonlinear-thermal-radiation and slip condition; Hamilton and Crosser's model. Waves Random Complex Media 1–22.
Wang, J., Xu, Y.-P., Qahiti, R., Jafaryar, M., Alazwari, M.A., Abu-Hamdeh, N.H., Issakhov, A., Selim, M.M., 2022. Simulation of hybrid nanofluid flow within a microchannel heat sink considering porous media analyzing CPU stability. J. Pet. Sci. Eng. 208, 109734.